Journal of Hydraulic Structures
J. Hydraul. Struct., 2021; 7(3):72-87
DOI: 10.22055/JHS.2022.39208.1196

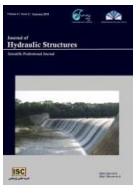

OPEN ACCESS

Application of Sluice Gate in Different Positions and Its Effect on Hydraulic Parameters in Free-Flow Conditions

Rasoul Daneshfaraz [1]
Hamidreza Abbaszadeh [2]
Pouya Gorbanvatan [2]
Moein Abdi [2]

Abstract

Underpass gates are hydraulic structures in which water moves under the gate. Here, different models of gate position including vertical, deflection to upstream and downstream of the channel with respect to the vertical axis and also oblique position concerning the transverse axis at angles of 10°, 20° and 30° was investigated numerically with FLOW-3D software. Also its effect on discharge coefficient (C_d) and hydrodynamic force applied to the gate was checked. The nested mesh was used for modeling. The results indicated that the statistical indices such as Absolute Error (AE), percentage Relative Error (RE%) and Root Mean Square Error (RMSE) in the RNG turbulence model were less than those of the k-ε, k-ω and Large Eddy Simulation (LES) and were more accurate compared to the experimental results. C_d in the same discharges increases with the increasing angle to the upstream of the channel compared to the vertical position. C_d is inversely related to increasing the angle of the gate relative to the vertical axis in the downward position. In the oblique position, C_d decreases with increasing angle to the transverse axis of the channel due to the increase in the area of flow through the gate. This increase in angle and area of the flow passing through the gate leads to a decrease in the upstream fluid depth, therefore, less hydrodynamic force is applied to the gate. The upward inclined gate tolerates less hydrodynamic force than the downward and oblique positions. The maximum value is related to the downward position.

Keywords: Sluice Gate, Stage-Discharge, Discharge Coefficient, Hydrodynamic Force, VOF

Received: 16 November 2021; Accepted: 8 January 2022

1. Introduction

Typically, the structure that determines the relationship between discharge and depth of flow in its vicinity is called the control structure. Among the flow control structures are sluice gates that have different shapes and functions hence they are used in different situations. To prevent

[1] Department of Civil Engineering, Faculty of Engineering, University of Maragheh, Maragheh, Iran, daneshfaraz@yahoo.com **(Corresponding Author)**
[2] Department of Civil Engineering, Faculty of Engineering, University of Maragheh, Maragheh, Iran.

water wastage, extreme care should be taken in controlling and distributing water in irrigation networks, and flow control structures such as gates should be selected correctly and following the conditions of each region. Principled design of such structures requires knowledge of hydraulic relationships and their calculation. Various researches have been done in the field of sluice gates to determine the discharge coefficient. Henry [1] deduced a diagram in which he expressed the changes in the discharge coefficient with the ratio of the upstream fluid depth to the gate opening for free-flow conditions. Rajaratnam and Subramanya [2] investigated the sluice gate discharge coefficient and confirmed (Henry [1]) results. Swamee [3] obtained the discharge coefficient of sluice gates as a function of upstream water depth and gate opening under free-flow conditions. Shivapur and Prakash [4] examined the placement of the sluice gates at different angles and provided a relationship to determine the amount of C_d. Nasehi Oskuyi and Salmasi [5] obtained the discharge coefficient of vertical sluice gates using Mathematica software. The results of their study were in good agreement with the diagram of Henry [1]. Mohammed and Moayed [6] investigated the effect of the gate edge shape and its deviation in the direction and opposite direction of flow. The results showed that C_d in the gate with an angle of 45 degrees in the flow direction and with a horizontal and sharp edge is 17.8% and 17% higher than the vertical gate, respectively. Daneshfaraz et al. [7] numerically investigated the effect of sluice gate edge shapes on flow characteristics. Their results indicated that the flow contraction coefficient for sharp edges and round-edge gates decreases when the ratio of gate opening to upstream specific energy is less than 0.4 and increases for the ratios greater than 0.4. Ashkan et al. [8] investigated the performance of consecutive sluice gates in regulating the discharge in channels using FLOW-3D software. Their results indicated that consecutive gates act with acceptable accuracy in the delivery of constant discharge in exchange for changes at upstream flow depth. Salmasi et al. [9] used experimental data and intelligence models to investigate C_d of inclined sluice gates. They concluded that the discharge coefficient increases with increasing gate placement angle.

In the case of vertical sluice gates, various numerical studies have been done including Ma et al. [10] which investigated the turbulence properties of hydraulic jumps using the standard k-ε turbulence model. Akoz et al. [11] performed experimental and numerical analysis of flow in sluice gates. Cassan and Belaud [12] examined the flow structure under sluice gates to confirm common assumptions about contraction coefficient and energy losses. Ghaderi et al. [13] numerically simulated free and submerged hydraulic jumps on different shapes of roughness in different roughness arrangements and different Froude number conditions in vertical sluice gate. Their results showed that the numerical model is well able to simulate the characteristics of the free and submerged jump. Ghaderi et al. [14] using FLOW-3D software investigated the effect of triangular roughness on jump characteristics, including longitudinal characteristics of streamlines, flow patterns in the cavity area, horizontal velocity profiles and velocity distribution in the direction of flow. Daneshfaraz et al. [15] examined the vertical gate flow in crescent-shaped contractions. The results showed that the effect of crescent-shaped contraction is greater than the sudden contraction of previous studies. A review of previous studies showed that so far, no study has been done on inclined and oblique gates using VOF method, and the report of the results of this type of gate is empty among scientific sources Also, carefully in the background of the research, there is a need to study the position of the gate and its effect on hydraulic capacity, corresponding discharge coefficients and hydrodynamic force on the gate at angles and type of gate placement. Therefore, considering the importance of the problem and how to respond FLOW-3D software in simulating the flow through the sluice gate, the necessity of sluice gate geometry, including an inclination to the upstream and downstream of the channel

and the oblique gates with different angles with respect to the vertical and transverse axis were investigated and compared with other researchers work.

2. Materials and methods

2.1. Flow governing equations

FLOW-3D software is a good alternative to physical models in solving fluid mechanics and hydrodynamics problems. This 3D software simplifies modeling and analysis of fluid behavior by using numerical methods. FLOW-3D software is an accurate and fast software that solves the difficult free-surface flow problems. The continuity and Navier-Stokes equations are discretized by FLOW-3D software to perform three-dimensional simulation of fluid motion. The continuity equation in a fluid stream is as follows (Flow Science Inc, [16]).

$$\frac{\partial \rho}{\partial t} + \frac{\partial}{\partial x_i}(\rho u_i) = 0 \tag{1}$$

where u_i is the velocity component of the direction i. FLOW-3D software solves the Navier-Stokes equations for three-dimensional flow analysis using the VOF on a networked field. The equations in the Cartesian coordinate system are obtained by the following equations (Flow Science Inc, [16]).

$$V_F \frac{\partial \rho}{\partial t} + \frac{\partial}{\partial x}(\rho u A_x) + R\frac{\partial}{\partial y}(\rho v A_y) + \frac{\partial}{\partial z}(\rho w A_z) = R_{SOR} + R_{DIF} \tag{2}$$

$$\frac{\partial u}{\partial t} + \frac{1}{V_F}\left(uA_x\frac{\partial u}{\partial x} + vA_y\frac{\partial u}{\partial y} + wA_z\frac{\partial u}{\partial z}\right) = -\frac{1}{\rho}\frac{\partial P}{\partial x} + G_x + f_x \tag{3}$$

$$\frac{\partial v}{\partial t} + \frac{1}{V_F}\left(uA_x\frac{\partial v}{\partial x} + vA_y\frac{\partial v}{\partial y} + wA_z\frac{\partial v}{\partial z}\right) = -\frac{1}{\rho}\frac{\partial P}{\partial y} + G_y + f_y \tag{4}$$

$$\frac{\partial w}{\partial t} + \frac{1}{V_F}\left(uA_x\frac{\partial w}{\partial x} + vA_y\frac{\partial w}{\partial y} + wA_z\frac{\partial w}{\partial z}\right) = -\frac{1}{\rho}\frac{\partial P}{\partial z} + G_z + f_z \tag{5}$$

In the above relations, u, v and w are velocity components, A_x, A_y and A_z are a fraction of the area associated with the flow, G_x, G_y and G_z are the body acceleration, f_x, f_y, and f_z are the viscosity acceleration in the directions of x, y and z, R_{SOR} is the mass source, R_{DIF} is the expression of turbulence, V_F is the fluid volume fraction, and P is the pressure. This equation is generally expressed as equation (6).

$$\rho\left(\frac{\partial u_i}{\partial t} + u_j\frac{\partial u_i}{\partial x_i}\right) = -\frac{\partial P}{\partial x_i} + B_i + \frac{\partial}{\partial x_j}\left[\mu\left(\frac{\partial u_i}{\partial x_j} + \frac{\partial u_j}{\partial x_i} - \frac{2}{3}\delta_{ij}\frac{\partial u_k}{\partial x_k}\right)\right] \tag{6}$$

where B_i is the volumetric force in direction i and μ is the dynamic viscosity of the fluid, ρ is the water density, x_i, x_j and x_k are the flow coordinates in the spatial direction i, j and k, respectively. δ_{ij} is Kronecker delta, where, if $i = j$ its value is equal to 1 otherwise, it has a zero value (Daneshfaraz et al. [17]).

2.2. Dimensional analysis

In Figure 1, the studied models are shown in different positions of the gates, including vertical, inclined to the upstream and downstream of the channel and oblique. Figure 1 shows the most significant parameters affecting the C_d and hydrodynamic force on the gate.

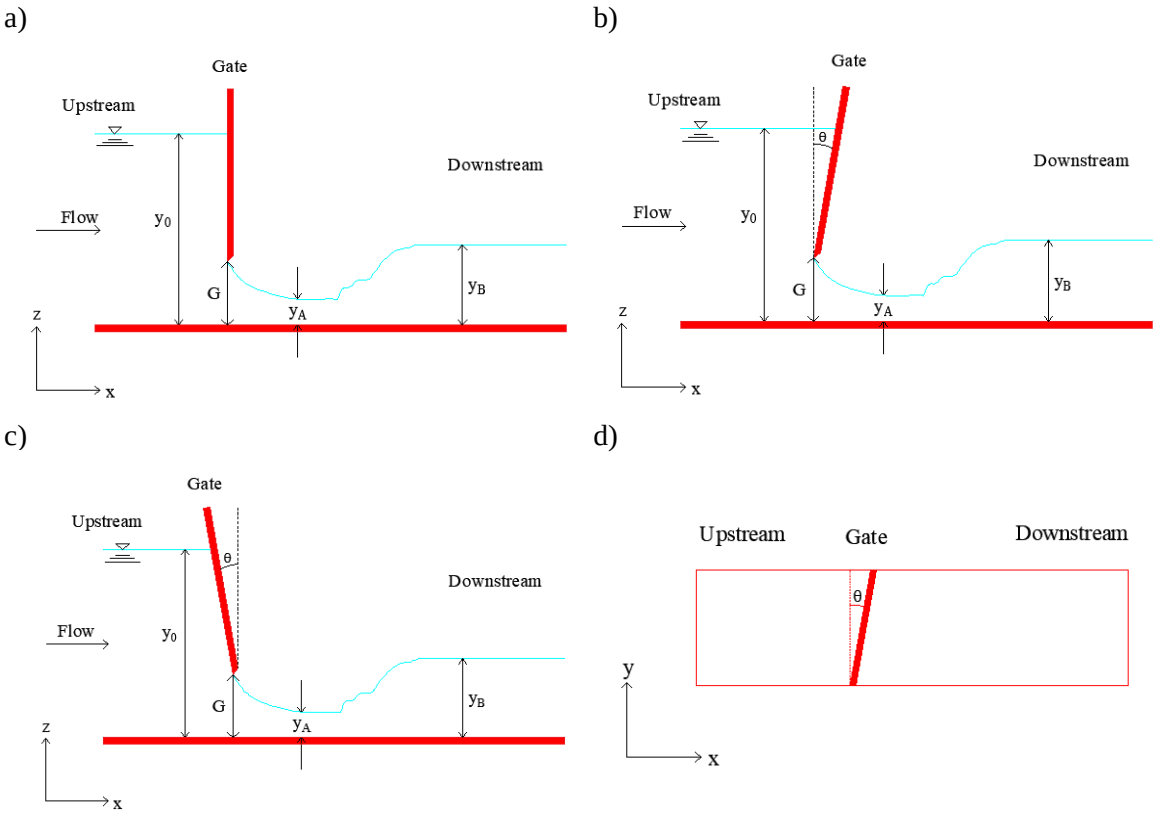

Figure 1. Schematic view of the gate a) Vertical position b) Downward inclined position c) Upward inclined position d) Oblique position.

The parameters affecting the flow rate through the inclined and oblique sluice gates can be shown as equation (7):

$$f_1(C_d.y_0.G.L.\rho.\mu.g.\theta) = 0 \tag{7}$$

In equation (7), C_d is the discharge coefficient (-), y_0 is the water depth upstream of the gate (L), G is the gate opening (L), L is the gate length (L), ρ is the water density (ML^{-3}), μ is the dynamic viscosity ($ML^{-1}T^{-1}$), g is the gravitational acceleration (LT^{-2}) and θ is the gate angle (-). Considering ρ, g and y_0 as iterative variables and using the π-Buckingham method, the dimensionless equation can be presented for the sluice gate discharge coefficient:

$$C_d = \frac{Q}{A\sqrt{2gy_0}} = f_2\left(\frac{y_0}{G}.\frac{y_0}{L}.Re.\theta\right) \tag{8}$$

In equation (8), R_e represents the dimensionless Reynolds number. In the present study, the flow is turbulent and $26361 \leq R_e \leq 60172$, so the effect of Reynolds number can be ignored (Daneshfaraz et al. [18]).

In equation (8), the area of the flow (A) through the oblique gate is calculated from equation (9):

$$A = LG \tag{9}$$

To calculate the subsurface level for the non-oblique gate state, in equation (9), instead of the L parameter, the channel width parameter, ie. W (L) is used.

The value of C_d in the vertical gate position is a function of the upstream water depth and gate opening, so the most significant parameter affecting it can be expressed as equation (10) (Swamee [3]):

$$C_d = f_1(y_0.G) \tag{10}$$

According to equation (11), the hydrodynamic force applied to the sluice gate can be calculated by writing the moment equation between sections 0 and A.

$$\frac{1}{2}\gamma y_0^2 - \frac{1}{2}\gamma y_A^2 - R = \rho q(V_A - V_0) \tag{11}$$

where q is the discharge per unit in width of the channel (L^2T^{-1}), γ is the specific weight ($ML^{-2}T^{-2}$), and R is the reaction force which is equal to the hydrodynamic force.

2.3. Definition of the solution network and boundary conditions

In this study, validation was performed using the experimental data of Shivapur and Prakash [4] for vertical gate, and then the simulations were continued for the studied models.

Table 1 presents the hydraulic and geometric characteristics of the studied models. Also, the three-dimensional geometry of the model and the mesh networks are shown in Figure 2.

Table 1. Hydraulic and geometric characteristics of the studied models

Hydraulic characteristics			
Upstream depth of the gate (m)	**Discharge (m^3/s)**	**Reynolds number (-)**	
0.06 – 0.3	0.0053 – 0.012	26361 - 60172	
Geometric characteristics			
Channel dimensions (m)	**θ (degree)**	**NO. Run**	
		Gate placement mode	**NO.**
2×0.5×0.2	Vertical – 10 – 20 – 30	Vertical	33
		Upward inclined position	33
		Downward inclined position	33
		Oblique position	33

a) b)

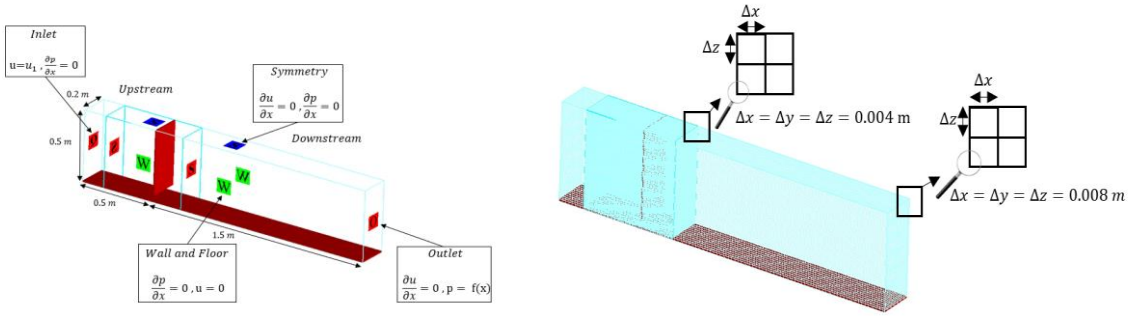

Figure 2- a) Three-dimensional geometry and boundary conditions b) Mesh networks

In this research, simulations have been performed using 2 nested mesh blocks with different dimensions. To achieve the optimal mesh, simulations were performed in 4 cases with different mesh dimensions and comparing results of numerical solution with experimental results, including upstream flow depth and C_d of the sluice gate. In the present study, the statistical indices of Absolute Error (AE), percentage Relative Error (RE%), Root Mean Square Error (RMSE) and the determination coefficient (R^2) were used to evaluate the model performance in simulation and compare its results with experimental results:

$$AE = \left|x_{exp} - x_{num}\right| \tag{12}$$

$$RE\% = \frac{AE}{x_{exp}} \times 100 \tag{13}$$

$$RMSE = \sqrt{\frac{\sum_{i=1}^{n}\left(x_{exp} - x_{num}\right)_i^2}{n}} \tag{14}$$

$$R^2 = \left(\frac{\sum_{I=1}^{n}\left(X_{exp} - \overline{X_{exp}}\right) \times \left(X_{num} - \overline{X_{num}}\right)^2}{\sqrt{\sum_{i=1}^{n}\left(X_{exp} - \overline{X_{exp}}\right)^2 \times \sqrt{\sum_{i=1}^{n}\left(X_{num} - \overline{X_{num}}\right)^2}}} \right) \tag{15}$$

In the above equations, *exp* and *num* represent the experimental and numerical results, *n* is the total number of data. The values of the equations (12, 13 and 14) when close to the number zero and the value of the equation (15) when closes to the number one indicates the high accuracy of the presented equations (Daneshfaraz et al. [15]).

Table 2. Optimal mesh selection

Test	Size of cells(m)	Total Mesh	Max Relative Error (%)		Mean Relative Error (%)		RMSE		R^2	
			y_0	C_d	y_0	C_d	y_0 (m)	C_d (-)	y_0	C_d
1	0.005,0.01	640000	26.72	16.82	21.04	12.64	0.0436	0.0776	0.966	0.652
2	0.0045,0.009	869352	9.89	5.35	5.24	2.76	0.0104	0.0184	0.993	0.904
3	**0.004,0.008**	**1250000**	**6.26**	**3.29**	**2.59**	**1.32**	**0.0054**	**0.0099**	**0.993**	**0.910**
4	0.0035,0.007	1868581	4.93	2.56	1.88	0.95	0.0038	0.0074	0.997	0.912

The results of the percentage Relative Error for the optimal mesh of 0.008 and 0.004 m are shown in Table 4 between the experimental and numerical data. According to Table 2 and investigating the statistical indicators, it was observed that test No.4 has desirable conditions in comparison with other test cases. The statistical indicators obtained from tests No.3 and 4 are very close to each other, therefore test No.3 is considered as the optimal mesh with mesh dimensions of 0.008 and 0.004 m to continue the simulation process of the studied models. While the difference between the total numbers of meshes between tests No.3 and 4 is 618581 meshes. The fluid range behind the gate and the hydrostatic pressure distribution was defined as the initial conditions. In selecting the boundary conditions, in the first mesh block, the volume flow rate and output boundary conditions are used for the input and end of the channel, respectively. Also, for the walls and floor, the boundary condition of the wall has been selected. For the upper, the symmetric boundary condition has been used. In addition, in the second mesh block, in order to be affected by the boundary conditions defined in the first mesh block, the symmetry boundary condition is defined for the input, output and upper boundary, and the wall condition is defined for the walls and the floor. Symmetry boundary condition considers the conditions outside the solution network similar to the conditions on the internal boundary of the network. Symmetry boundary condition acts as a mirror that reflects all the flow distribution to the other side. Another application of this type of boundary condition is at the free surface of the fluid. When the boundary condition on the boundary Z_{max} is considered symmetry (Ghaderi et al. [19]), the conditions above the fluid surface are considered to be infinitely similar to the atmospheric conditions until the flow doesn't reach this boundary. Another application of this boundary condition, which is used as a solution field in problems of more than one cube network, is to use it on the interlocking faces of two separate solution networks (mesh blocks). In this way, the flow characteristics at the boundary of the first network are assigned to the second network without change. In the present study, two nested block meshes have been used. In order to affect the second mesh block from the boundary conditions defined in the first mesh block, the symmetry boundary condition has been used.

2.4. Turbulence models

To select the turbulence model simulations were performed with four RNG, k-ε, k-ω and LES models. Finally, the RNG turbulence model was selected to continue the simulations. There are numerous reasons for choosing this model such as reliability in answering various problems, accurate solution of equations, high accuracy in showing the details of the flow and review of previous studies (Ghaderi et al. [13], Ghaderi et al. [19]). Also, the comparison of the simulation results of the turbulence models mentioned in Table 3 shows that the RNG turbulence model has less error than other turbulence models and its results are closer to the experimental data. While other models have results close to the experimental results.

Table 3. Numerical solution results for different turbulence models

Turbulence Model	Max Relative Error (%)		MRE		RMSE		R^2	
	y_0	C_d	y_0	C_d	y_0 (m)	C_d (-)	y_0	C_d
RNG	**6.26**	**3.29**	**2.59**	**1.32**	**0.0054**	**0.0099**	**0.993**	**0.910**
k-ε	6.65	3.50	3.10	1.58	0.0060	0.011	0.990	0.864
k-ω	6.89	3.63	3.40	1.74	0.0067	0.012	0.988	0.828
LES	6.45	3.39	2.82	1.44	0.0055	0.0103	0.992	0.891

3. Results and Discussion

In this study, the experimental results of Shivapur and Prakash [4] were used for validation. According to Figure 3, it can be seen that there is a good agreement between the results of the experimental and numerical solution. So that the Mean Relative Error percentages, Mean Absolute Error, Root Mean Square Error between experimental and numerical solution results for the upstream depth of the gate are 2.59%, 0.0045 m and 0.0054 m, respectively, and these values are 1.32%, 0.0078 and 0.0099 for C_d, respectively. Table 4 shows the calculation of the percentage Relative Error between each experimental and numerical data for the discharge coefficient and water depth upstream of the gate in different discharges for nested mesh with sizes of 0.008 and 0.004 meters.

a) b)

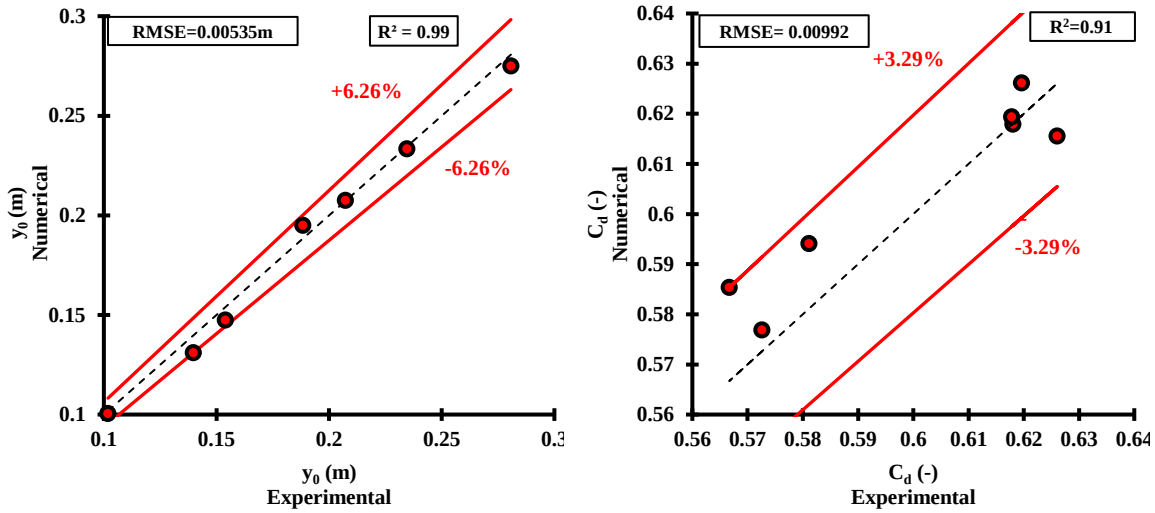

Figure 3. Comparison of a) Upstream water depth b) C_d obtained from the results of experimental and numerical solution

Table 4. Percentage relative error between experimental and numerical results for C_d and y_0 at different discharges

Q (m^3/s)	C_d (-) Experimental	C_d (-) Numerical	RE (%)	y_0 (-) Experimental	y_0 (-) Numerical	RE (%)
0.00648	0.5726	0.5768	0.74	0.102	0.100	1.46
0.00751	0.5667	0.5853	3.29	0.140	0.131	6.26
0.00808	0.5811	0.5941	2.23	0.154	0.147	4.31
0.00963	0.6261	0.6155	1.68	0.188	0.195	3.46
0.00997	0.6181	0.6179	0.03	0.207	0.207	0.06
0.01060	0.6178	0.6194	0.25	0.235	0.233	0.50
0.01163	0.6196	0.6261	1.05	0.281	0.275	2.07

According to the initial and boundary conditions, the numerical solution starts non-permanently and continues until the flow reaches a steady state until the solution becomes stable (Figure 4-a). According to Figure 4-b, the changes in the upstream water level are shown for the discharge of 0.0075 m^3/s. It is observed that over time, these changes have diminished and the water level has stabilized at a certain depth.

a)

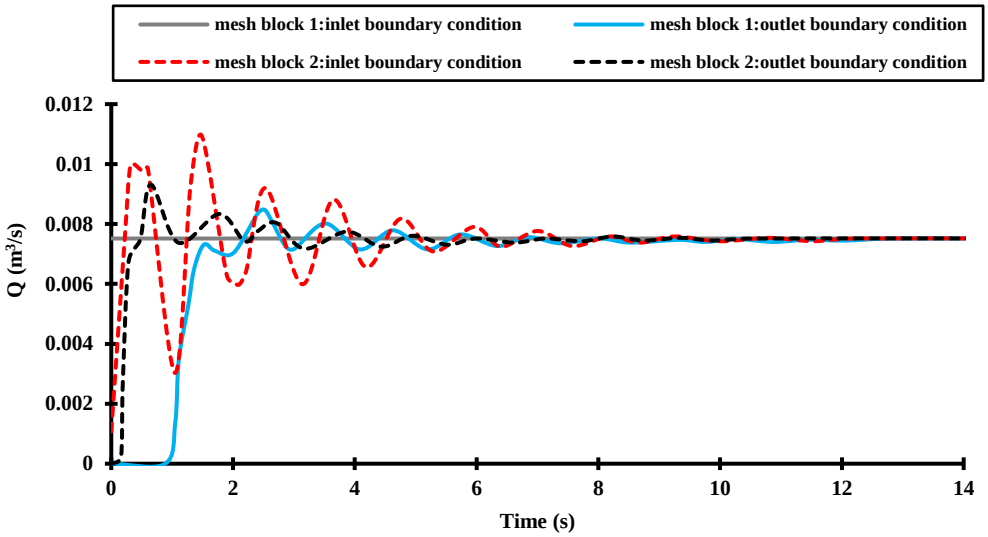

b)

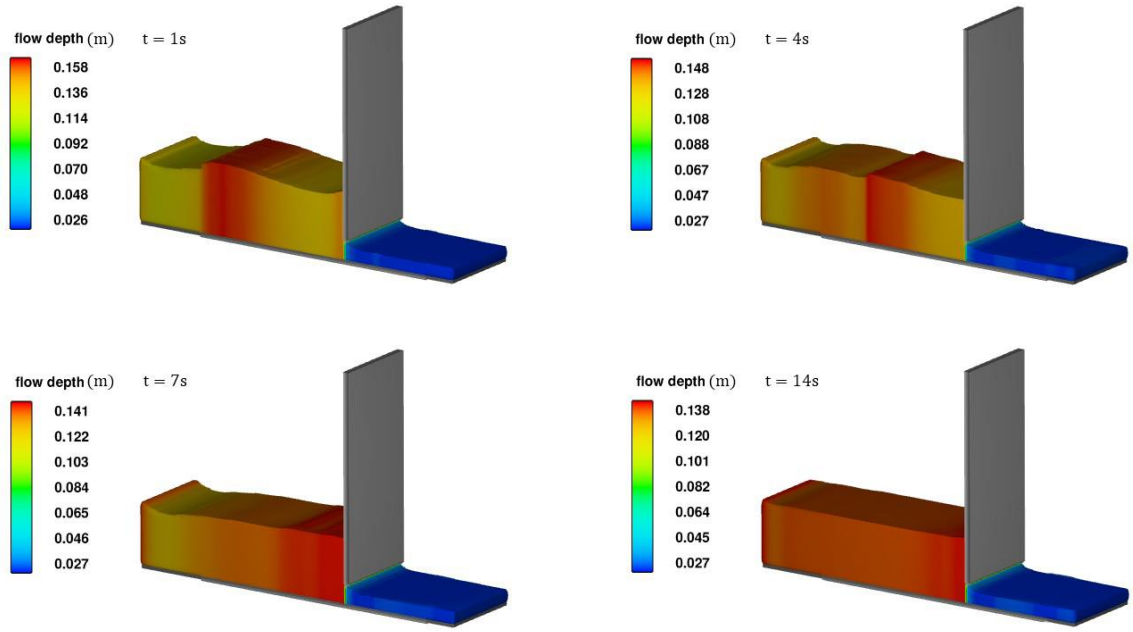

Figure 4. a) Discharge-time hydrograph diagram b) Three-dimensional figure of flow at different times

3.1. Upward inclined gate discharge coefficient

Figure 5-a shows the stage-discharge diagram for the vertical and inclined sluice gates with angles of 10°, 20° and 30°. At the same discharge, when the sluice gate is at an angle of 30°, the upstream water depth has the lowest value, and the highest value is related to the vertical position. In other words, by increasing the angle, the depth upstream of the gate decreases. The reason for this can be pointed to the position of the gate so that as the angle increases, the flow through the gate converges and the flow lines tend more to the outlet of the gate. It also reduces the upstream flow turbulence near the gate. This factor leads to more flow passing through the sluice gate (Figure 6). Figure 5-b shows the discharge coefficient changes in different positions relative to the vertical axis. In the upward position of the gate, the discharge coefficient is directly related to θ and increases with increasing the θ and vice versa. So that C_d of the gate with an angle of 30˚ is more than 20˚, 10˚ and vertical positions, respectively. On average, the sluice gate discharge coefficient in 30˚ is 5.88%, 12% and 16.05% higher than the 20˚, 10˚ and vertical positions, respectively. The flow area through the gate is constant at all angles. Also, the position of the gates leads to a change in the depth upstream of the gate, which is the most important parameter affecting the discharge coefficient.

a) b)

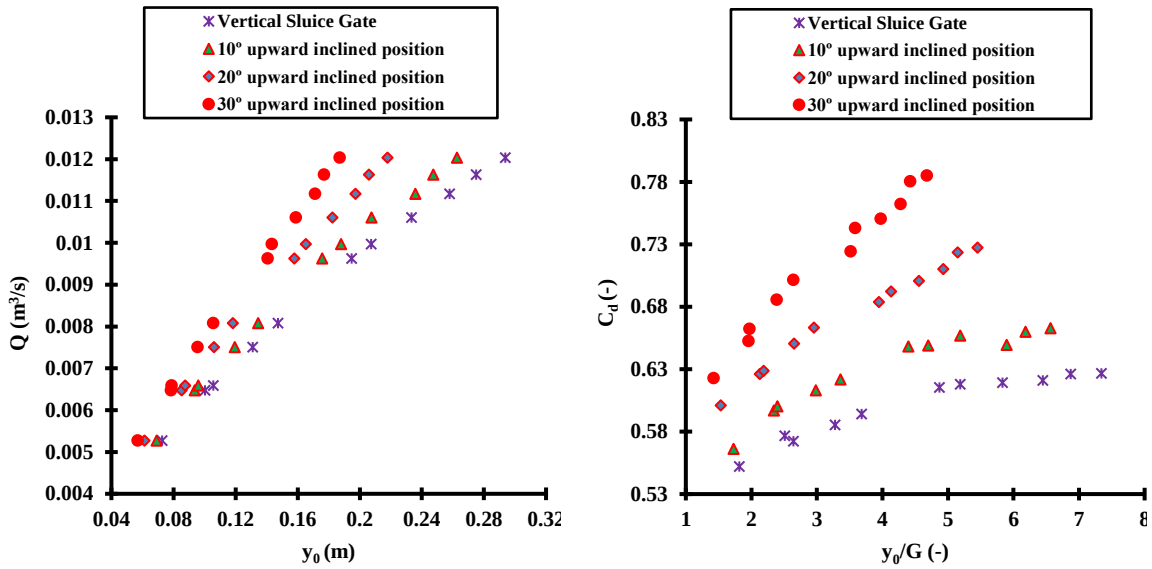

Figure 5. Diagram a) Stage-discharge b) C_d at different angles of sluice gate

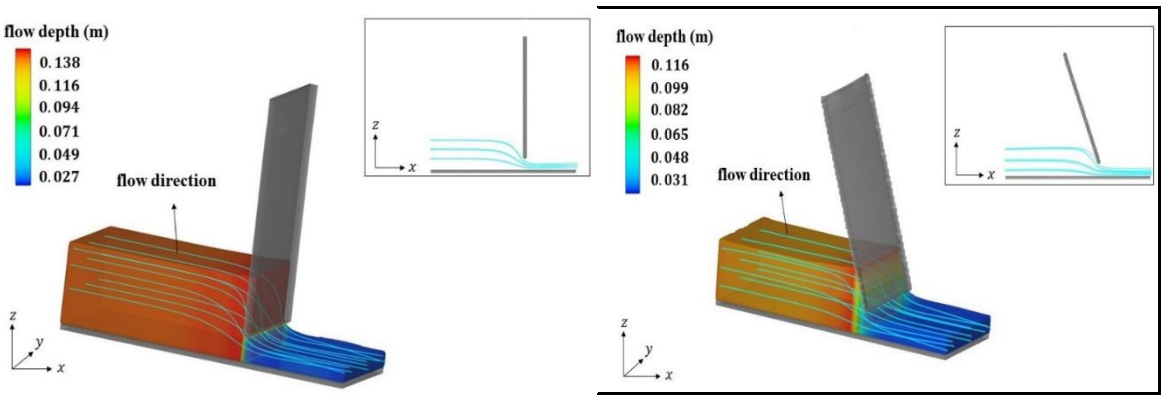

Figure 6. Upstream flow depth and flow lines at the same discharge in different gate position

3.2. Downward inclined gate discharge coefficient

Figure 7-a shows the stage-discharge diagram for a sluice gate with angles of 10˚, 20˚ and 30˚. As can be seen, increasing θ relative to the vertical axis causes a slight increase in the depth upstream of the gate concerning the vertical position, which leads to a decrease in the discharge coefficient (Figure 7-b). On average, the gate discharge coefficient in the vertical position is 0.58%, 1.49% and 2.18% higher than the gate with angles of 10˚, 20˚ and 30˚, respectively.

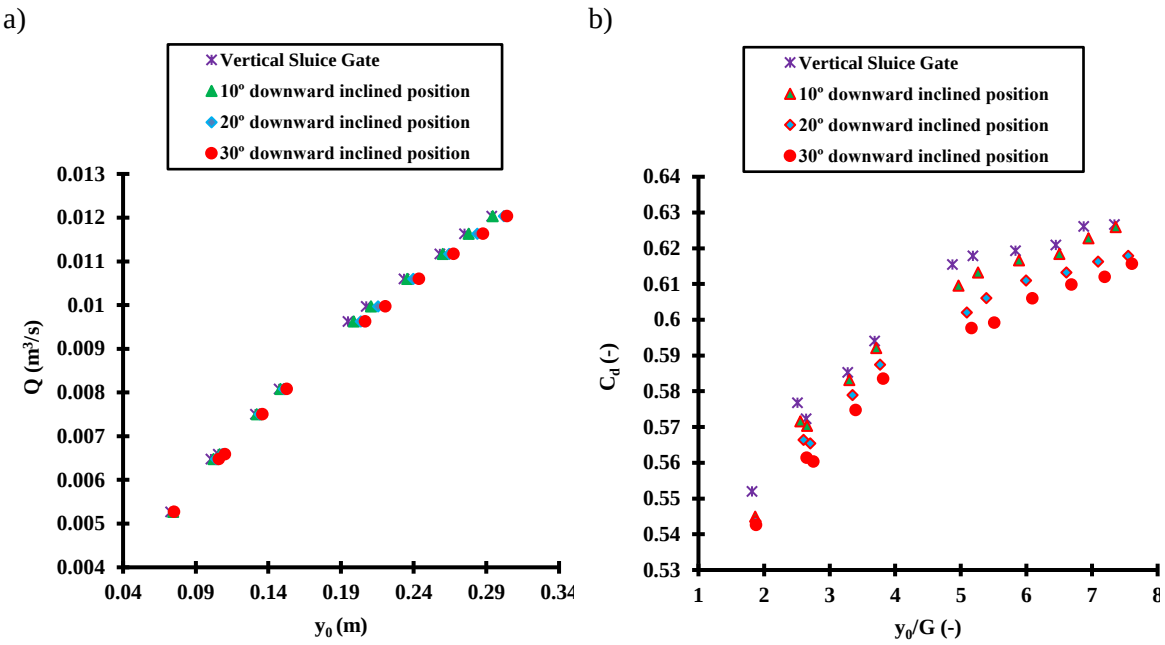

Figure 7. Diagram a) Stage-discharge b) Discharge coefficient at different angles of sluice gate

3.3. Oblique gate discharge coefficient

Figure 8-a is presented for the vertical and the oblique gates relative to the transverse axis with angles of 10°, 20° and 30°. The angle of the oblique gate is inversely related to the upstream water depth. So that increasing the angle leads to reducing the water depth. According to Figure 8-a, the value of C_d increases with increasing y_0/G. In Figure 8-a, the highest C_d value

is related to the vertical gate and the lowest is related to the gate with an angle of 30˚. As the angle increases, the length of the gate becomes longer than the vertical gate, which leads to an increase in the area of flow through the gate, hence the discharge coefficient reduces at greater angles. Also, this type of gate placement causes the output flow to be asymmetric under and downstream of the gate. So that, the depth and flow velocity on the sides of the gate are different from each other. Imbalance in hydraulic parameters reduces the discharge coefficient. The effect of gate length is shown in Figure 8-b. This diagram shows the effect of gate length on upstream depth and discharge coefficient. In a constant discharge and different gate lengths, the discharge coefficient of the gate with a shorter length is greater than the discharge coefficient with a longer length.

a) b)

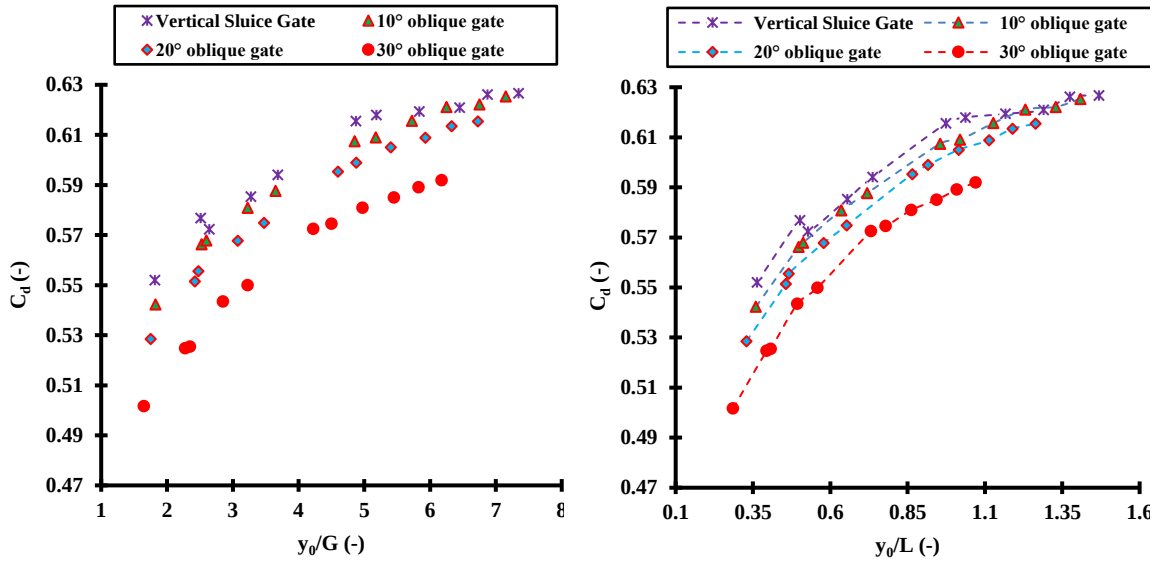

Figure 8. Diagram a) Stage-discharge b) Discharge coefficient at different angles of sluice gate placement

Table 5 shows the minimum, maximum and average discharge coefficient for all gate placement modes in this and previous studies. On average, the values of C_d for the upward inclined gate positions with an angle of 10˚, 20˚ and 30˚ are 4.58%, 10.81% and 16.05% more than the vertical position, respectively. Also, for downward gate positions with an angle of 10˚ is 0.58% for gates with angles of 20˚ and 30˚, are 1.49% and 2.18% less than the vertical position, which shows that the downward position does not have much effect on discharge coefficient. On average, for oblique gate positions with angles of 10°, 20° and 30°, 0.93%, 2.91% and 7.08% are less than the vertical position. Given that the discharge coefficient in the upward position is higher than other models, so the gate in this position can be considered the best position to increase C_d.

Table 5. Comparison of discharge coefficient of the present study with previous studies

Gate Cases		Discharge Coefficient																		
		Present study			Rajaratnam & Subramanya [2]			Rajaratnam [20]			Nago [21]			Hager [22]			Gate Cases	Shivapur & Prakash [4]		
		Max	Min	Avr	Max	Min	Avr	Max	Min	Avr	Max	Min	Avr	Max	Min	Avr	-	Max	Min	Avr
	Vertical	0.63	0.55	0.60	0.63	0.58	0.61	0.64	0.60	0.62	0.59	0.53	0.55	0.59	0.53	0.55	Vertical	0.63	0.52	0.61
Inclined to UP	10º	0.66	0.57	0.63	-	-	-	-	-	-	-	-	-	-	-	-	15º	0.68	0.58	0.66
Inclined to UP	20º	0.73	0.60	0.67	-	-	-	-	-	-	-	-	-	-	-	-	30º	0.74	0.61	0.70
Inclined to UP	30º	0.79	0.62	0.72	-	-	-	-	-	-	-	-	-	-	-	-	45º	0.83	0.64	0.78
Inclined to DS	10º	0.63	0.54	0.60	-	-	-	-	-	-	-	-	-	-	-	-	-	-	-	-
Inclined to DS	20º	0.62	0.54	0.59	-	-	-	-	-	-	-	-	-	-	-	-	-	-	-	-
Inclined to DS	30º	0.62	0.54	0.58	-	-	-	-	-	-	-	-	-	-	-	-	-	-	-	-
Oblique	10º	0.63	0.54	0.60	-	-	-	-	-	-	-	-	-	-	-	-	-	-	-	-
Oblique	20º	0.62	0.53	0.58	-	-	-	-	-	-	-	-	-	-	-	-	-	-	-	-
Oblique	30º	0.59	0.50	0.56	-	-	-	-	-	-	-	-	-	-	-	-	-	-	-	-

Table 6. Hydrodynamic force on the gate

NO	Q (m^3/s)	q (m^3/s-m)	R (kg/m)									
			Gate Cases									
			Vertical position	10º upward inclined position	20º upward inclined position	30º upward inclined position	10º downward inclined position	20º downward inclined position	30º downward inclined position	10º oblique position	20º oblique position	30º oblique position
1	0.0052	0.0264	0.684	0.406	0.295	0.222	0.995	1.254	1.584	0.975	0.950	0.862
2	0.0065	0.0324	1.860	1.186	1.036	0.727	2.557	2.504	2.746	2.417	2.374	2.036
3	0.0066	0.0330	2.238	1.263	1.128	0.772	2.757	2.824	3.072	2.587	2.509	2.279
4	0.0075	0.0375	4.087	2.597	2.037	1.455	4.428	4.984	5.415	4.393	4.359	3.993
5	0.0080	0.0404	5.556	3.689	2.815	1.990	5.970	6.762	7.319	6.028	5.978	5.521
6	0.0096	0.0481	11.215	7.604	6.412	4.746	12.402	14.348	18.705	12.083	11.207	10.585
7	0.0099	0.0499	13.084	9.159	7.219	4.808	14.257	16.348	19.322	14.115	12.671	12.268
8	0.0106	0.0530	17.593	11.810	9.349	6.433	18.714	21.135	23.598	17.898	15.968	15.423
9	0.0111	0.0559	21.444	16.886	11.395	7.818	23.741	26.611	29.168	21.927	19.859	18.934
10	0.0116	0.0582	25.963	18.707	12.524	8.290	27.600	33.501	34.823	26.310	23.019	21.957
11	0.0120	0.0602	29.398	21.706	14.475	9.660	31.523	40.919	41.396	29.967	26.515	24.984

Table 6 shows the hydrodynamic force applied to the sluice gate in all different models and discharges. Examination of the results indicated that increasing the discharge rate increases the hydrodynamic force on the gate, which is also due to the increase in the upstream depth of the gate. This increase in depth increases the pressure and force on the gate. Comparison of the results showed that the hydrodynamic force on the gate has the lowest value in the upward gate position and the highest value related to the downward position. So that by increasing the angle with respect to the vertical axis upstream of the channel, the hydrodynamic force decreases. In the case of oblique gates, the upstream depth decreases with increasing angle and therefore the hydrodynamic force decreases.

4. Conclusion

In the present study, the hydraulic parameters of the sluice gate, including discharge coefficient (C_d) and hydrodynamic force on the gate in different positions, including upward and downward deviation and oblique position were investigated using FLOW-3D software. The simulations were performed in the discharge range of 0.0053 to 0.012 m^3/s. The RNG turbulence model showed acceptable results in terms of accuracy in model simulation and the results obtained between the numerical solution and experimental in comparison with other turbulence models such as k-ε, k-ω and LES. To validate the model and achieve the desired mesh, several simulations with different mesh dimensions were performed. By examining the results of statistical indicators with different mesh dimensions, mesh blocks with nested mesh dimensions of 0.8 and 0.4 cm were selected as the optimal mesh. The results showed that the upward inclined gate has a higher discharge coefficient compared to other gate models. The maximum C_d is for an upward inclined gate with an angle (θ) of 30° with a quantity of 0.79. On average, the gate discharge coefficient in the 30° upward position is 5.88%, 12% and 16.05% higher than the 20° and 10° upward and vertical positions, respectively. The results showed that the hydrodynamic force on the gate decreases in the upward inclined position with increasing θ. This value is inverted for the downward inclined gate position and increases with increasing θ. So that, the hydrodynamic force on the gate in the vertical position is less than the gate with an angle of 30° to the downstream of the channel. The discharge coefficient for the downward inclined gate does not change significantly with increasing θ. In the case of oblique gate, increasing θ leads to an increase in the area of flow through the gate and also decreases the upstream fluid depth, so the discharge coefficient was lower than in the vertical position. 30° upwards inclined gate showed 16.67% and 22.22% higher discharge coefficient than the vertical and 30° downward gate positions, respectively.

References

1. Henry H. R, (1950). Discussion on "Diffusion of Submerged Jets, "by Albertson, M. L. et al., Trans. Am. Society Civil Engrs, 115: 687.
2. Rajaratnam N, Subramanya K, (1967). Flow Equation for the Sluice Gate. Journal of the Irrigation and Drainage Division, 93(3): 167-186.
3. Swamee PK, (1992). Sluice Gate Discharge Equations. Journal of Irrigation and Drainage Engineering, 118(1): 56-60.
4. Shivapur AV, Shesha Prakash MN, (2005). Inclined Sluice Gate for Flow Measurement. ISH Journal of Hydraulic Engineering; 11(1): 46-56.
5. Nasehi Oskuyi N, Salmasi F, (2012). Vertical Sluice Gate Discharge Coefficient, Journal of Civil Engineering and Urbanism, 2(3): 108-114.
6. Mohammed A, Moayed K, (2013). Gate Lip Hydraulics under Sluice gate. Modern Instrumentation. 2(1): 16-19. Doi: 10.4236/mi.2013.21003.
7. Daneshfaraz R, Ghahramanzadeh A, Ghaderi A, Joudi AR, Abraham J, (2016). Investigation of the Effect of Edge Shape on Characteristics of Flow under Vertical Gates. Journal of American Water Works Association, Doi.org/10.5942/jawwa.2016.108.0102.
8. Ashkan F, Daneshfaraz R, ghaffarinik A, Gahramanzadeh A, Minaei O, (2019). Numerical Investigation of the Successive Sluice Gates Performance in Regulating Flow Rate through Channels Using Flow-3D Software. Water and Soil Science, 29(4): 85-96.
9. Salmasi F, Nouri M, Sihag P, Abraham J, (2021). Application of SVM, ANN, GRNN, RF, GP and RT Models For Predicting Discharge Coefficients of Oblique Sluice Gates Using Experimental Data. Water Supply, 21(1): 232-248.
10. Ma F Hou Y, Prinos P, (2001). Numerical Calculation of Submerged Hydraulic Jumps. Journal of Hydraulic Research, 39:5, 493-503, DOI: 10.1080/00221686.2001.9628274.
11. Akoz M, Kirkgoz M, Oner A, (2009). Experimental and Numerical Modeling of a Sluice Gate Flow. J. Hydraul. Res., 47(2): 167-176.
12. Cassan L, Belaud G, (2010). Experimental and Numerical Studies of the Flow Structure Generated by a Submerged Sluice Gate. Conference: 1st European IAHR Congress At: Edinburgh, U K.
13. Ghaderi A, Dasineh M, Aristodemo F, Ghahramanzadeh A, (2020). Characteristics of free and submerged hydraulic jumps over different macroroughnesses. Journal of Hydroinformatics, 22 (6): 1554–1572.
14. Ghaderi A, Dasineh M, Aristodemo F, Aricò C, (2021). Numerical Simulations of the Flow Field of a Submerged Hydraulic Jump over Triangular Macroroughnesses. Water, 13(5): 674.
15. Daneshfaraz R, Aminvash E, Abbaszadeh H, (2021). Numerical Simulation of Energy Dissipation in Crescent-Shaped Contraction of the Flow Path. Iranian Journal of Soil and Water Research. 52(5): 1299-1314. Doi: 10.22059/ijswr.2021.318989.668895.
16. Flow Science Inc. 2016 FLOW-3D V 11.2 User's Manual, Santa Fe, NM, USA; 2016.

17. Daneshfaraz R, Norouzi R, Abbaszadeh H, (2021). Numerical Investigation on Effective Parameters on Hydraulic Flows in Chimney Proportional Weirs. Iranian Journal of Soil and Water Research. 52(6): 1599-1616. Doi: 10.22059/ijswr.2021.322751.668944.
18. Daneshfaraz R, Aminvash E, Esmaeli R, Sadeghfam S, Abraham J, (2020). Experimental and Numerical Investigation for Energy Dissipation of Supercritical Flow in Sudden Contractions. Journal of Groundwater Science and Engineering, 8(4): 396-406.
19. Ghaderi A, Abbasi S, Abraham J, Azamathulla HM, (2020). Efficiency of Trapezoidal Labyrinth Shaped stepped spillways. Flow Measurement and Instrumentation, Doi.org/10.1016/j.flowmeasinst.2020.101711.
20. Rajaratnam N, (1977). Free Flow Immediately Below Sluice Gates. Journal of the Hydraulics Division 103(4): 345-351.
21. Nago H, (1978). Influence of Gate Shapes on Discharge Coefficients. Proceedings of Japan Society of Civil Engineers. pp. 59-71.
22. Hager WH, (1999). Underflow of Standard Sluice Gate. Experiments in Fluids 27(4): 339-350. Doi:10.1007/s003480050358.